

LETTER TO THE EDITOR

Double photoexcitation of $1P^0$ states in helium

D Wintgen† and D Delande‡

† Fakultät für Physik, Hermann-Herder-Strasse 3, 79104 Freiburg, Federal Republic of Germany

‡ Laboratoire de Spectroscopie Hertzienne de l'Ecole Normale Supérieure, Tour 12, Université Pierre et Marie Curie, 4, place Jussieu, F-75252 Paris Cedex 05, France

Received 27 May 1993

Abstract. For P^0 states of helium we formulate a Schrödinger equation in perimetric coordinates in which the rotational coupling is already pre-diagonalized. Expansions in near-complete basis sets and complex scaling techniques allows the determination of highly accurate *ab initio* parameters for doubly excited resonant states and photo cross sections. The results are in excellent agreement with recent high-quality experimental data.

The helium atom is the simplest atom for which an analytic solution of the Schrödinger equation is impossible. With its two valence electrons, it serves as the prototype system for the study of electron correlations in neutral atoms. Because of its formal simplicity, it is the focus of current interest, both experimentally (see Domke *et al* 1991, 1992 and references therein) and theoretically (Fano 1983, Herrick 1983, Rost and Briggs 1991, Ezra *et al* 1991). Moreover, the classical dynamics of this three-body problem is known to be mainly ergodic. A major open problem is to understand the consequences on the quantum properties of the system when the two electrons are simultaneously highly excited.

This spectral region of high excitations of both electrons is of particular interest and is characterized by many open decay channels and a high density of autoionizing resonant states. After the initial pioneering experiment by Madden and Codling (1963) and its theoretical interpretation (Cooper *et al* 1963), it took nearly three decades until highly improved experimental data became available (Domke *et al* 1991, 1992). The theoretical understanding has also improved in recent years and several sets of approximate quantum numbers are now available to describe certain states (Herrick 1983, Rost and Briggs 1991, Lin 1984, Richter *et al* 1992). Nevertheless, highly accurate calculation of resonance parameters and cross sections is still a formidable task and the high quality of the latest experiments (Domke *et al* 1992) challenges the theory to calculate adequate cross sections for comparisons.

It is the aim of this paper to present such calculations which became possible by merging recent theoretical and computational developments (Richter *et al* 1992, Delande *et al* 1991) as described below. With the new techniques at hand, we are able to compute relevant resonance parameters nearly routinely with an accuracy which is several orders of magnitude better in cases where published data are available. The present results not only signal a computational development, they also uncover physical effects hitherto unidentified in data analyses, e.g. avoided crossings and interactions of Rydberg series converging to the same threshold.

The non-relativistic Hamiltonian of the helium atom with nuclear charge $Z = 2$ is given by (atomic units used)

$$H = \frac{p_1^2 + p_2^2}{2} - \frac{Z}{r_1} - \frac{Z}{r_2} + \frac{1}{r_{12}}. \quad (1)$$

The electron positions are given by r_j , $j = 1, 2$ and the distance between the electrons is r_{12} . For simplicity of notation, we set the nuclear mass in (1) to infinity, but the corrections due to mass polarization terms are straightforward to incorporate in the theory outlined below. The conclusions drawn from the present results for infinite mass remain valid for finite mass M typical of nuclei, and the energies (and total decay widths) are only affected to order of $1/M$. The total angular momentum L is conserved and its separation from the equations of motion reduces the number of degrees of freedom from six to four. Expressing the Jacobi coordinates $R = r_1 - r_2$, $r = \frac{1}{2}(r_1 + r_2)$ in spherical $R = (R, \Theta, \Psi)$ and cylindrical $r = (\rho, \zeta, \varphi)$ coordinates respectively, the total two-electron wavefunction is given by

$$\psi_{LM}(r, R) = \sum_{-L \leq T \leq L} D_{MT}^{L*}(\Psi, \Theta, \varphi) \Phi_T(R, \rho, \zeta). \quad (2)$$

The rigid top wavefunctions D_{MT}^L describe the overall rotation of the three-body complex (Brink and Satchler 1968) and are eigenfunctions of L^2 with eigenvalues $L(L+1)$ and eigenfunctions of L_z with eigenvalues M and T in the space- and body-fixed frames, respectively. Rotational coupling induces mixing of the different T subspaces, but for the particular symmetry of P^0 states this coupling can be pre-diagonalized,

$$\begin{aligned} \psi_{L=1,M} = & [(\zeta + R/2)D_{M,0}^{1*} + \rho(D_{M,-1}^{1*} - D_{M,1}^{1*})/\sqrt{2}] \Phi(R, \rho, \zeta) \\ & \pm [(\zeta - R/2)D_{M,0}^{1*} + \rho(D_{M,-1}^{1*} - D_{M,1}^{1*})/\sqrt{2}] \Phi(R, \rho, -\zeta). \end{aligned} \quad (3)$$

The plus (minus) sign corresponds to singlet (triplet) states. Note that the dependence of the total wavefunction on the Euler angles (Ψ, Θ, φ) is already fully accounted for by this pre-diagonalization which reduces the remaining number of degrees of freedom to three.

The internal motion is described by the wavefunction Φ . For its evaluation, we transform to perimetric coordinates (x, y, z) (Pekeris 1958) and expand Φ in a Sturmian-type basis set $\{\phi_n(u) = L_n(u) \exp(-u/2)\}$,

$$\Phi(x, y, z) = \sum_{nmk} c_{nmk} \phi_n(\alpha x) \phi_m(\beta y) \phi_k(\gamma z). \quad (4)$$

The scaling parameters α, β, γ are free to choose. For the present calculations we used $\alpha = 2\beta = 2\gamma$ which are the convenient parameters for intra-shell states in the limit $Z \rightarrow \infty$. The expansion (4) has already been profitably used for calculations of S states of Coulombic three-body systems (Pekeris 1958, Richter and Wintgen 1991, Rost and Wintgen 1992). For P states the derivation of the matrix equation of the Hamiltonian (1) requires some straightforward but very tedious analytic operations, the derivation of which will be published elsewhere. Nevertheless, the final result is simple and all required matrix elements are given in closed form. In addition, most of them vanish due to selection rules so that the Hamiltonian matrix is of sparse banded structure and allows for efficient diagonalization.

We use the method of complex rotation (Reinhardt 1982, Ho 1983) to calculate highly accurate energies and decay widths of doubly-excited resonant states. In addition, (complex)

Table 1. Various properties of doubly-excited resonances of the different $N = 2$ series for infinite nuclear mass. Energies E and widths Γ are given in au and 10^{-4} au, respectively. q is the Fano shape parameter for transitions from the ground state.

K_n	$-E$	$\Gamma/2$	q
0 ₂	0.693 134 920	6.866 2482	-2.77
1 ₃	0.597 073 804	0.019 2251	-4.25
0 ₃	0.564 085 188	1.505 9423	-2.58
-1 ₃	0.547 092 709	0.000 0523	-23.4
1 ₄	0.546 493 256	0.010 1443	-3.32
0 ₄	0.534 363 144	0.641 7335	-2.55
-1 ₄	0.527 616 338	0.000 0007	-132
1 ₅	0.527 297 769	0.004 9105	-3.31

dipole-transition matrix elements $d = \langle \psi_g | \hat{e} \cdot \mathbf{r} | \Phi \rangle$ from the (complex rotated) helium ground state $|\psi_g\rangle$ are evaluated which allows the calculation of cross sections (Delande *et al* 1991) and the direct determination of the Fano (resonance) shape parameters $q = -\Re d / \Im d$ (Broad 1992). Here we report on photo cross sections for linear polarization \hat{e} .

For the diagonalization of the complex symmetric eigenvalue problem of the rotated Hamiltonian (1), we used a Lanczos algorithm described recently (Delande *et al* 1991). We checked the convergence of the eigenvalues and of the transition matrix elements by increasing the basis size up to $N = n + k + m = 38$, corresponding to matrix dimensions (bandwidths) up to 10660 (1395). Due to the band structure of the matrices and the efficient diagonalization algorithm used, such calculations require only a couple of minutes on a modern RISC workstation. The wavefunction of the ground state was calculated under inclusion of $N = 46$ shells, which gives an accuracy up to 17 significant digits for the energy.

For not too highly doubly-excited states, the $^1P^o$ spectrum of the helium atom can be characterized as follows. A set of $2N - 1$ different Rydberg series converges to each hydrogenic energy level $E = -2/N^2$ of the He^+ ion. As long as N is small ($N < 5$), Rydberg series converging to different thresholds do not overlap and the structure of the spectrum is rather simple. The series can be labelled conveniently with an index K , $-(N - 1) \leq K \leq N - 1$, which measures the angular correlation between the electrons (Herrick 1983, Rost and Briggs 1991), i.e. $\langle \cos \angle(\mathbf{r}_1, \mathbf{r}_2) \rangle \simeq K/N$. Close to threshold, the symmetry character of the different Rydberg series is governed by the degree of polarization of the inner electron and the label K equals the difference of the parabolic quantum numbers of the inner electron (Rost and Briggs 1991). A further index n counts the states in the different series. In an independent-particle picture, n would yield the principal quantum number of the outer electron. For one-photon transitions from the ground state the $K = N - 2$ series is dominantly excited.

Despite the (seemingly) simple structure of this part of the spectrum, it was only very recently (Domke *et al* 1992) that all series of resonances converging to even the lowest, i.e. $N = 2$, threshold were identified experimentally. From the theoretical point of view, accurate predictions—for example for decay widths, transition strengths and shape parameters—do not exist for all these different series. Using the above method, we were able to derive these parameters. In table 1 we list values for the positions and the decay widths of the lowest resonances of each series together with the shape parameters for transitions from the ground state. The values given are converged to all digits quoted. We emphasize that the most accurate calculations were unable to give any reliable estimate of the widths (Ho 1991) and oscillator strengths of the $K = -1$ series. The results of Ho (1991) agree

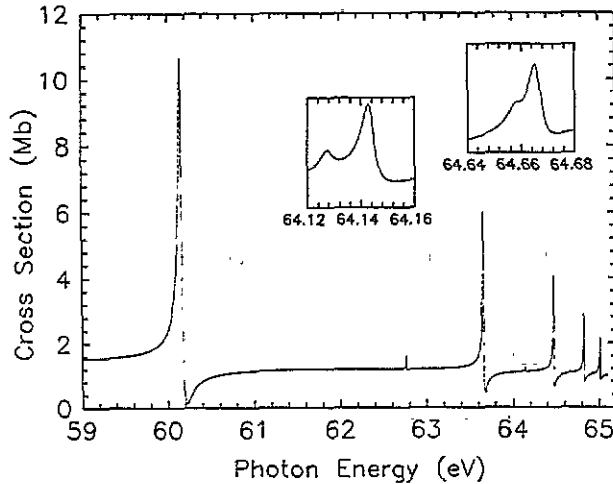


Figure 1. Photo cross section for energies close to the $N = 2$ threshold. The data are smoothed with a Lorentzian of width 5.6 meV. The dominant structures belong to the $K = 0$ series. The weak structures at 64.14 and 64.66 meV, belonging to the $K = \pm 1$ series, are shown separately on an enlarged scale. The dominant part of the weak structures comes from the $K = +1$ states and the sub-dominant part from the $K = -1$ states.

Table 2. Transition frequencies (in eV) of the weak $N = 2$ series for finite nuclear mass (${}^4\text{He}$). The experimental transition frequencies are from Domke *et al* (1992).

K_n	$\hbar\omega_{\text{theor}}$	$\hbar\omega_{\text{exp}}$
1 ₃	62.7581	62.7580
-1 ₃	64.1179	64.1189
1 ₄	64.1342	64.1353
-1 ₄	64.6478	64.6485
1 ₅	64.6564	64.6574
-1 ₅	64.9062	64.9071
1 ₆	64.9111	64.9123

with ours to within the accuracy cited by Ho. For further references of calculated data see, e.g., Domke *et al* (1992).

The photo cross section for transitions from the ground state into the series is shown in figure 1. To simulate the experimental conditions of Domke *et al* (1992) we smoothed the spectrum with a Lorentzian of width 5.6 meV. In addition to the well known dominant $K = 0$ series (Gersbacher and Broad 1990), states belonging to the $K = \pm 1$ series are weakly excited but they are hardly visible within the scale of the figure. The $K = -1$ series is so weak that its first members have been observed only very recently (the $(2p, nd)$ series in Domke *et al* (1992)). The series is nearly degenerate with the $K = +1$ series. For its first members the cross sections are plotted separately in figure 1. A very good agreement is obtained with the experiment (see figure 2 in Domke *et al* (1992)).

Even though the form of the experimental cross section is nicely reproduced there is a slight shift of ≈ 10 meV in the excitation energies. Consideration of the finite mass of the nucleus in the Hamiltonian (1) largely accounts for this discrepancy. For the weak series the transition frequencies are tabulated in table 2 together with the recent high-precision experimental data. Except for the lowest state of the $K = +1$ series (which is isolated in energy) the theoretical values are systematically smaller by ≈ 1 meV. The overlapping

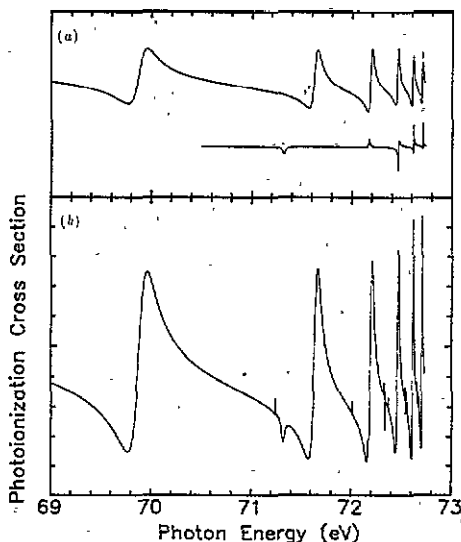


Figure 2. Infinite-resolution photo cross section near the $N = 3$ threshold, (b). A smooth background term has been subtracted. The dominant structures arise from the $K = \pm 1$ Rydberg series. These contributions are shown separately in (a), where the upper curve is $K = +1$ and the lower curve is $K = -1$.

contributions of higher lying resonances in the experimental data make it difficult to extract the precise resonance positions. The remaining discrepancy between theory and experiment may be related to this uncertainty, but the error is anyway four times smaller than the width of the synchrotron light source used in the experiments.

As long as interference effects between different Rydberg series can be neglected, the series are characterized by smooth quantum defect parameters (Friedrich 1992). Strong deviations from this rule indicate significant mixing with other states. This happens for large values of $N > 5$ where the Rydberg series converging to different thresholds overlap and the spectrum becomes complicated. The effects of these mixings on the photo cross section have been demonstrated in a recent experiment (Domke *et al* 1991). For Rydberg series converging to the same threshold, interference effects have not been seen so far, neither in experiments nor in theoretical calculations.

Table 3. Transition frequencies from the ground states (in eV) for the lowest states of the different $N = 3$ Rydberg series (infinite nuclear mass). The leftmost column belongs to the dominant series in the cross section and the transition strengths become weaker to the right.

$K = 1$	$K = -1$	$K = 2$	$K = 0$	$K = -2$
69.882				
71.635	71.318	71.233		
72.191	72.169	72.009	71.731	
72.458	72.461	72.364	72.260	72.335
72.609	72.613	72.554	72.503	72.536
72.702	72.705	72.667	72.638	72.656

In figure 2 we demonstrate, however, that such mixings do indeed occur between $K = \pm 1$ states of the $N = 3$ Rydberg series. Part (b) shows the infinite-resolution cross section near the $N = 3$ threshold. The main structure is caused by the $K = 1$ series,

while the resonance at 71.3 eV belongs to the $K = -1$ series and is energetically well separated from the first two resonances of the $K = 1$ series at 69.9 and 71.6 eV. The very narrow resonances with small transition strengths belong to other K series and are invisible in the finite-resolution experimental spectrum of Domke *et al* (1991). However, as noted by the experimentalists, no other member of the $K = -1$ series seems to be visible. The reason for this is that the $K = \pm 1$ series have an 'avoided' crossing near 72.5 eV. This is demonstrated in table 3, where we list the transition frequencies of the different K series. Whereas, in the beginning, the $K = -1$ resonances are below the $K = 1$ ones, the situation changes for higher members of the series. Near 72.5 eV, the resonances are so close together that their contributions overlap. We emphasize that interactions of the Rydberg series with states converging to others thresholds can be excluded: Apart from the (small) avoided crossing the quantum defects of the states vary only weakly with energy and the lowest state converging to the $N = 4$ threshold is energetically well separated (see figure 3 below).

An advantage of the complex rotation method is that it is nevertheless possible to separate the different contributions since each resonance contributes with a single term to the cross section (Delande *et al* 1991). This is shown in part (a) of the figure, where we plot the $K = \pm 1$ series separately. Whereas the dominant part of the cross section is still coming from the $K = 1$ states (upper curves) the contribution of the $K = -1$ states (lower curve) indicates a strong admixture of both series. This can be seen by the increased transfer of oscillator strength into the $K = -1$ series and by the different shapes of the resonances in the same series. Both effects are a signature of *complex resonances* (Friedrich 1992) arising from interference between different Rydberg series.

Finally, we show in figure 3 the photo cross section near the $N = 4$ threshold. The data are smoothed to compare with the experimental data of Domke *et al* (1991, their figure 2). The dominant structure comes from the $K = 2$ series, for which the first quantum defects are $\mu_n = 1.319, 1.287, 1.344, 1.384, 1.415, 1.440$ ($n = 4, \dots, 9$). Note that the μ_n have a rather strong energy dependence. They are the precursors of the pseudo-resonant jump (Friedrich 1992) by unity in the quantum defect caused by the lowest $N = 5$ state (Wintgen 1993) which is located *below* the $N = 4$ threshold at 75.58 eV.

In addition to the strong series, some weak structures are visible in figure 3 near 74.15, 74.86, and 75.13 eV. They belong to the next dominant series $K = 0$, which is also visible

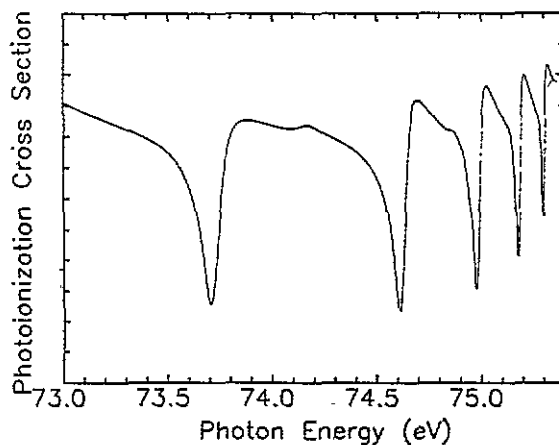


Figure 3. Photo cross section near the $N = 4$ threshold. The data are smoothed with a Lorentzian of width 5.6 meV and a smooth background term has been subtracted. The dominant structure is caused by the $K = 2$ resonances, the weak structure by the $K = 0$ states.

in the experimental data of Domke *et al* (1991) even though the authors did not focus on its existence. All the other series have very small transition strengths and they are hardly visible in a finite-resolution spectrum.

Using a diabatic-by-sector hyperspherical method, Tang *et al* (1992) have computed very recently the photo cross section for the $N = 5$ series and observed a similar effect, namely a weak series visible in the experimental spectra, though unnoticed by the experimentalists. An advantage of our method is to reproduce all the resonances, including extremely narrow ones (see figure 2), in a single calculation. Furthermore, once the resonance data are given the cross section can be calculated efficiently on an arbitrary fine energy grid. In contrast, a diabatic-by-sector method requires evaluation of the wavefunctions and of the cross section at regularly spaced energies and can miss very narrow resonances (compare, e.g., with the figures in Tang *et al* (1992).

In summary, we solved a Schrödinger equation for P^0 helium states in which the rotational coupling is pre-diagonalized and which depends only on three internal (perimetric) coordinates. The complex rotation method is used to calculate resonance parameters and photo cross sections by expansions in near-complete basis sets. The results are in excellent agreement with recent experiments. For the first time, we could show that avoided crossings of Rydberg series converging to the same threshold may occur. This symmetry-breaking leads to characteristic effects for resonance parameters and cross sections. A weak resonance series contributes to the $N = 4$ cross sections which should become visible in slightly improved experiments or data analyses.

This work was supported by the Deutsche Forschungsgemeinschaft (SFB 276). Laboratoire de Spectroscopie Hertzienne de l'École Normale Supérieure et de l'Université Pierre et Marie Curie is Unité Associée 18 du Centre National de la Recherche Scientifique. We are grateful to J S Briggs for fruitful discussions.

References

- Brink D M and Satchler G R 1968 *Angular Momentum* (Oxford: Clarendon)
- Broad J T 1992 Private communication
- Cooper J W, Fano U and Prats F 1963 *Phys. Rev. Lett.* **10** 518
- Delande D, Bommier A and Gay J C 1991 *Phys. Rev. Lett.* **66** 141
- Domke M, Remmers G and Kaindl G 1992 *Phys. Rev. Lett.* **69** 1171
- Domke M *et al* 1991 *Phys. Rev. Lett.* **66** 1306
- Ezra G S, Richter K, Tanner G and Wintgen D 1991 *J. Phys. B: At. Mol. Opt. Phys.* **24** L413
- Fano U 1983 *Phys. Rep.* **46** 97
- Friedrich H 1992 *Theoretical Atomic Physics* (Berlin: Springer)
- Gersbacher R and Broad J T 1990 *J. Phys. B: At. Mol. Opt. Phys.* **23** 365
- Herrick D R 1983 *Adv. Chem. Phys.* **52** 1
- Ho Y K 1983 *Phys. Rep.* **99** 1
- 1991 *Z. Phys. D* **21** 191
- Lin C D 1984 *Phys. Rev. A* **29** 1019
- Madden R P and Codling K 1963 *Phys. Rev. Lett.* **10** 516
- Pekeris C L 1958 *Phys. Rev.* **112** 1649
- Reinhardt W P 1982 *Ann. Rev. Phys. Chem.* **33** 223
- Richter K, Briggs J S, Wintgen D and Solov'ev E A 1992 *J. Phys. B: At. Mol. Opt. Phys.* **25** 3929
- Richter K and Wintgen D 1991 *J. Phys. B: At. Mol. Opt. Phys.* **24** L565
- Rost J M and Briggs J S 1991 *J. Phys. B: At. Mol. Opt. Phys.* **24** 4293
- Rost J M and Wintgen D 1992 *Phys. Rev. Lett.* **69** 2499
- Tang J-Z, Watanabe S, Matsuzawa M and Lin C D 1992 *Phys. Rev. Lett.* **69** 1633
- Wintgen D 1993 to be published